*The paper was published in the proceedings of the 6th International Conference on Geotechnical and Geophysical Site Characterization and was edited by Tamás Huszák, András Mahler and Edina Koch. The conference was originally scheduled to be held in Budapest, Hungary in 2020, but due to the COVID-19 pandemic, it was held online from September 26th to September 29th 2021.*

# Evaluation of bearing capacity and in situ shear strength using the screw plate load test in clay and silt

Ø. Blaker
*Norwegian Geotechnical Institute, Oslo, Norway, oyvind.blaker@ngi.no*

D. J. DeGroot
*University of Massachusetts, Amherst, MA, USA, degroot@umass.edu*

J. T. DeJong
*University of California, Davis, CA, USA, jdejong@ucdavis.edu*

**ABSTRACT:** Recent studies show that silts are sensitive to sampling disturbance, and that the effects of sampling can be adverse and opposite of those typically observed for clays. Silts often exhibit a tendency for dilative behavior upon undrained triaxial shear. As a result, the interpreted shear strength is highly dependent on which failure criterion is selected but there is limited guidance or consensus on what criterion represents the relevant in situ shear strength for design applications. To this end, in situ Screw Plate Load Tests (SPLT) have been conducted at Halden, Norway, to investigate the bearing capacity and behavior of the silt and clay deposits under field loading, and uncertainties associated with undrained/drained/partially-drained conditions. Normalized penetration velocity indicates that the SPLTs were likely partially-drained in the silt unit and undrained in the clay unit. This information was used to back-calculate estimates of the in situ strengths for comparison with laboratory tests conducted on undisturbed specimens from both soil units.

**Keywords:** silt; clay; triaxial test; screw plate load test; bearing capacity.

## 1. Introduction

An increasing number of geotechnical projects involving silt has sparked a series of research efforts to better understand the fundamentals of this intermediate soil, the effects of sampling disturbance and uncertainties associated with undrained/drained/partially-drained conditions. For sands and clays, deformation and strength parameters can be evaluated in situ through well-established correlations with measured or derived parameters from cone penetration tests with pore pressure measurements (CPTU), dilatometer tests (DMT), self-boring pressuremeter tests (SBP), or back-calculated and interpreted from plate load tests (PLT). The CPTU, for example, can be used to estimate undrained shear strength ($s_u$), effective stress friction angle ($\phi'$), constrained modulus ($M$) and small strain shear modulus ($G_{max}$) of a soil with depth, and to estimate axial pile capacity ($Q_{ult}$) from the cone resistance ($q_c$).

Methods for interpretation of laboratory and in situ tests in silt have not seen the same developments or conclusive research as for clays and sands, and there are still large uncertainties associated with in situ behavior and appropriate geotechnical parameters for practical engineering design in this soil type. Partial drainage effects may have a significant effect on sample quality, the interpreted soil behavior type and soil properties from in situ and laboratory testing. For example, results from "twitch" testing at variable penetration rates have demonstrated how CPTU measurements change with normalized penetration velocity ($V$), expressed as:

$$V = vD/c_h \tag{1}$$

where $v$ = rate of penetration; $D$ = penetrometer diameter; and $c_h$ = coefficient of horizontal consolidation. $V$ > 10 – 100 have been suggested to be indicative of fully undrained conditions, while fully drained conditions typically occurs for $V$ < 0.05 – 0.01 [1-3]. Penetrometer measurements conducted under $V$ = 0.05 - 10 may therefore be affected by partial drainage.

Furthermore, recent studies demonstrated that silts are particularly sensitive to sampling disturbance, and that the effects of tube sampling on engineering properties can be adverse and opposite of those typically observed for clays [4]. Tube samples of silt often exhibit a tendency for dilative behavior and strain hardening upon undrained triaxial shear in compression and, as a result, the undrained shear strength of this material cannot be readily interpreted at the conventional peak shear stress as for soft structured clays [4-8]. The shear strength of the material depends on the criterion selected for interpretation and there is limited guidance or consensus on what criterion most accurately represents the relevant in situ shear strength for design.

As sampling of silt has traditionally been considered challenging, and quantitative assessment of sample quality using clay-based criteria is highly questionable in this soil type, in situ loading tests were considered attractive for evaluation of bearing capacity and shear strength. Marsland [9] used PLT data to back-calculate undrained shear strength of stiff, fissured London clay, showing that the large-scale undrained shear strength was significantly lower than that measured in small undrained triaxial compression test (CAUC) specimens. A variation of the PLT, the SPLT uses a single flight helical screw to advance from ground level without the need for a pre-augered borehole, thus retaining the overburden stress [10]. This configuration was adopted and used to evaluate compressibility of different sands and the influence of preconsolidation stress on sand deformability by Schmertmann [11] and Dahlberg [12], respectively. The device has also been successfully used in a number of different clays [13-17], but only a few results have been conducted in silt. Janbu and Senneset [18] and Sandven [19] report incremental loading SPLTs (i.e., fully drained conditions) conducted at a silt site in Stjørdal, Norway for evaluation of in situ compressibility of the deposit.

This paper presents results of three SPLTs conducted at the National GeoTest Site for silt in Halden, Norway. It investigates load-deformation behavior in the clayey silt and underlying clay units, interpretation of engineering parameters and compares the measured bearing capacities with calculated base unit resistance for an equivalent diameter closed end pile.

## 2. Methods

### 2.1. Sampling

Soil samples were collected at the Halden, Norway research site [8] using the Sherbrooke block sampler [20] in location HALB04, the NGI 54 mm inner diameter (ID) composite piston sampler [21] in location HALB03 and the Gregory Undisturbed Sampler (GUS), a hydraulic fixed piston sampler, manufactured by Acker Drill Company, PA, USA in location HALB07. All locations are presented on the map in Figure 1.

### 2.2. Field equipment

The screw plate equipment consisted of a single helix flight auger (Figure 2) with $D$ = 160 mm (Area, $A$ = 200 cm$^2$) and a 45 mm pitch. The plate was founded in ductile cast iron (EN-GJS-500) by Ulefoss Foundry, Norway based on a model by Strout [22]. The screw plate was positioned directly in front of a custom-made down-hole hydraulic jack and double-rod configuration described by Janbu and Senneset [18]. The outer 42.5 mm outer diameter (OD) steel rods provided torque during installation and reaction from the jack to the drill tower of the Georigg 607 (Geotech AB, Sweden) drill rig during static loading. A simple load frame was positioned between the outer rod and drill rig and allowed access to the top of the 27 mm OD center rods. The unloaded center rods provided direct measurement of the plate displacement using two Mitutoyo Digimatic ID-C 0.001/50.8 mm deformation indicators mounted on an independent reference beam. An Enerpac P392 hand pump and a 64 MPa GDS high pressure volume controller provided hydraulic pressure to the closed system through a 400 MPa capacity hydraulic hose connected to the jack positioned directly behind the screw plate. Hydraulic cylinder pressure to plate stress ($q_p$) conversions were calibrated in the laboratory using an Interface (Interface Inc., Scottsdale, AZ, USA) 250 kN load cell.

The screw plate was carefully installed by rotation from ground level to target depth ($z$) by the drill rig. The rate of penetration during installation was adjusted to equal the pitch of the screw plate (i.e. about 45 mm per 360° rotation) in order to minimize disturbance to the surrounding soil. The Enerpac pump and GDS volume controller were connected to the hydraulic hose, the plate pressure was set equal to the in situ vertical effective stress and the equipment was allowed to rest for about 15 min to allow equalization of installation pore pressures near the screw plate. Displacement gauges were zeroed, and continuous rate of deformation testing was conducted using the GDS pump. A GDS flow rate of about 40 mm$^3$/s was typically used, providing a displacement rate of about 1.33 mm/min (0.5$D$/hr). Readings of cylinder pressure and plate displacement (s) at fixed time intervals ($t$) were recorded to a displacement of about $s$ = 0.2$D$. After completion of a test, the reference beam and deformation indicators were dismounted, and the system carefully vented to atmospheric pressure. The oil reservoir was vented and the hydraulic cylinder, typically fully extended after testing, was reset to its original position using the drill rig. Finally, the pumps were disconnected, and the screw plate advanced to the next test depth.

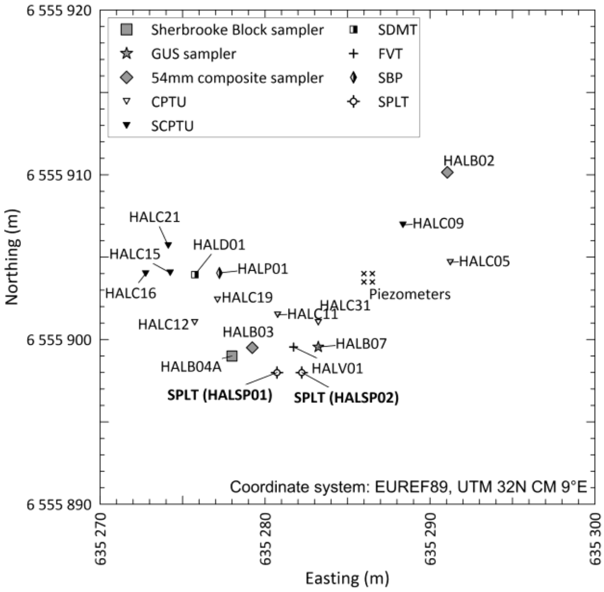


**Figure 1.** In situ testing and sampling locations at Halden. SPLTs were conducted in HALSP01 and HALSP02.

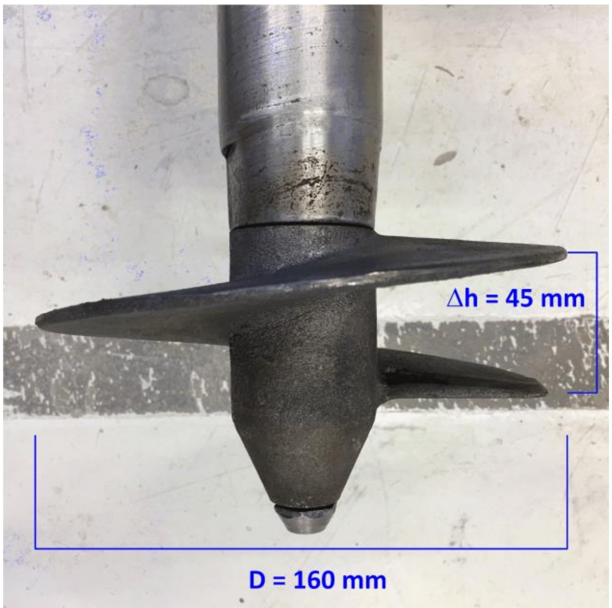


**Figure 2.** Screw plate with diameter D = 160 mm and pitch of 45 mm used at the Halden GeoTest Site.

## 2.3. Triaxial testing

Triaxial specimens were prepared by trimming of Sherbrooke block and GUS specimens using the procedures described by Lacasse and Berre [23] and Ladd and DeGroot [24]. During back pressure saturation the test specimens were first subjected to an isotropic stress (cell pressure) equal to the estimated value of the initial negative pore pressure (suction) within the specimen. The porous filter stones were initially dry. At the initial isotropic stress, de-aired water was flushed through the porous stones and any tendency for volume change was prevented by adjusting the cell pressure until a stable condition was reached. Following this stage, backpressure was applied and all $B$ values, which were measured at the end of the consolidation phase, were ≥ 97%. All specimens were anisotropically consolidated to the best estimate in situ vertical effective stress, $\sigma'_{v0}$ and horizontal effective stress $\sigma'_{h0}$ using an assumed $K_0 = 0.5$ [8]. All specimens were allowed to creep for 12 to 24 hours prior to undrained shear testing performed at a strain rate of 0.5 – 1.4 %/hr. The total radial stress was kept constant while the total axial stress was increased in compression (CAUC). All stress measurements were corrected for membrane resistance and changes in specimen area [25].

## 2.4. Analysis

### 2.4.1. Ultimate bearing capacity from SPLT

Three methods were used to assess the ultimate bearing capacity, $q_{ult}$ from the SPLT stress-displacement curves:

- 0.1$B$ method – ultimate bearing stress limited by a relative displacement, typically 10% of the footing width or pile diameter, B [26, 27]. In this case, 10% of the screw plate diameter, D, i.e. $q_{ult} = q_{0.1D}$.
- Tangent intersect – bearing stress corresponding to a distinct change in plate displacement, i.e. intersection of initial and final tangent slope of stress - settlement plot [28], i.e. $q_{ult} = q_{TI}$.
- Curve fitting – ultimate bearing capacity extrapolated using an exponential curve intersecting the bearing stress, $q_x$ and $q_y$ at 0.015$D$ and 0.02$D$, respectively [15], i.e. $q_{ult} = q_{KP}$.

Other methods are available, e.g. the Log-Log method [29], but were considered inappropriate for the interpretation of the load tests described in this paper. For all methods listed above the displacement at failure ($s_f$) were taken as the displacement corresponding to $q_{ult}$.

### 2.4.2. Pile ultimate unit base resistance

A deeply embedded screw plate ($z/D$ > 33) may be compared to the base of a circular closed end pile (CEP) with equivalent diameter and area. The ultimate base resistance of a pile is expressed as [30]:

$$Q_{b,ult} = q_{b,ult} A_b \qquad (2)$$

where $q_{b,ult}$ = the ultimate unit base resistance and $A_b$ = area of the pile base. The ultimate unit base resistance of a pile tip equivalent to that of the screw plate ($D$ = 160 mm) was assessed using a number of methods, including:

- the classical bearing capacity equation (disregarding the $0.5\gamma' D N_\gamma^*$ term due to its small relative contribution), i.e.:

$$q_{b,ult} = N_c^* s_u + N_q^* \sigma'_{v0} \qquad (3)$$

  where $N_c^*, N_q^*, N_\gamma^*$ = dimensionless bearing capacity factors for deep foundations, including necessary shape and depth factors; $s_u$ = undrained shear strength; and $\gamma'$ = effective unit weight of soil [31-33].
- CPTU-based methods, including:
  - Purdue-CPT [27],
  - NGI-05 [34, 35],
  - ICP-05/MTD-1996 [36, 37], and
  - UWA-05/UWA-13 [38, 39].

All CPTU-based design methods are summarized by Han, et al. [40].

### 2.4.3. Shear strength

Undrained shear strength from CAUC tests on clay specimens were assessed at peak shear stress, i.e. $s_{uC} = 0.5(\sigma_1 - \sigma_3)_{max}$. For silt specimens displaying dilative type behavior during undrained shear, and thus, no peak shear stress, $s_{uC}$ was evaluated using the following strength criteria [41]:

- maximum deviator stress, $(\sigma_1 - \sigma_3)_{max}$;
- an assigned limiting vertical strain, $\varepsilon_{vf}$;
- state of zero excess shear induced pore pressure at failure $\Delta u_f = 0$, which is equivalent to Skempton's A parameter at failure equal to zero, $A_f = 0$;
- point at which the effective stress path first reaches the failure envelope, defined by the $K_f$ line;
- maximum obliquity, $(\sigma'_1/\sigma'_3)_{max}$;
- maximum shear induced pore pressure, $u_{max}$.

Undrained shear strength assessed from the screw plate load tests were back-calculated using:

$$s_u = q_{ult}/N_c^* \qquad (4)$$

## 3. Test program and site description

Three SPLTs were performed, one at a depth of 11.3 m in borehole HALSP01, and one each at 11.3 and 17.8 m depths in borehole HALSP02 (Figure 2) at the Norwegian GeoTest Site (NGTS) for silt. The site is located in Halden, Norway, approximately 120 km south of Oslo and has been well characterized [see 8] by combining the

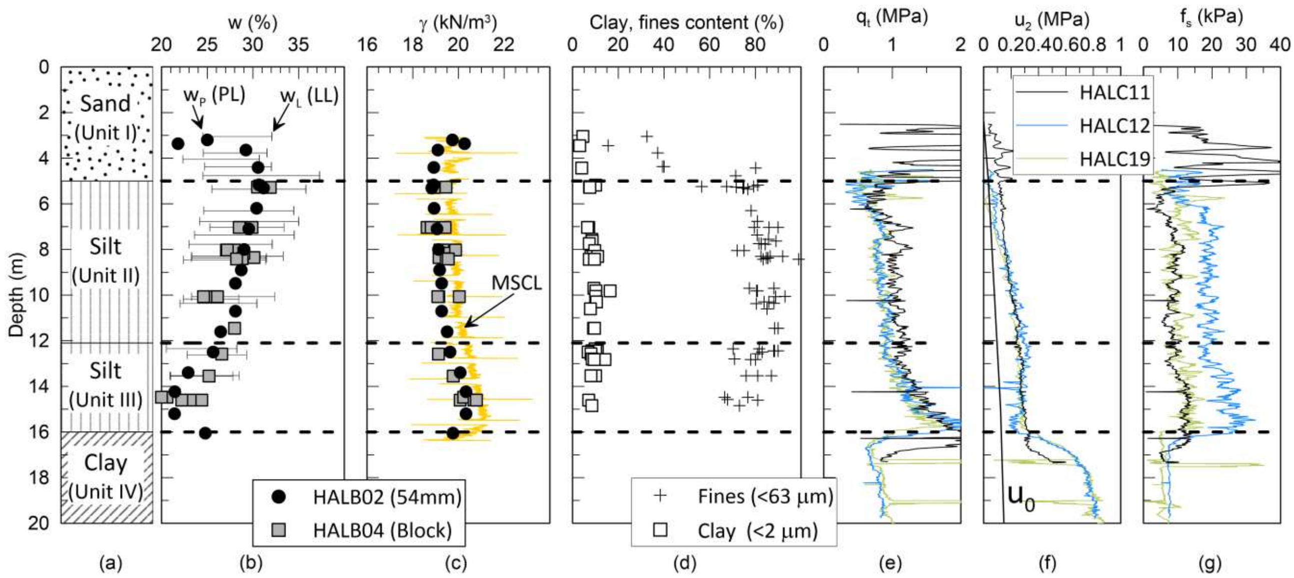


**Figure 3.** Classification and CPTU characteristics of the Halden research site; (a) Soil Units, (b) natural water content and Atterberg limits, (c) total unit weight, and (d) clay particle and fines content, (e) corrected cone resistance, $q_t$, (f) pore pressure, $u_2$, and (g) sleeve friction, $f_s$. Modified from Blaker, et al. [8].

results of a number of geological, geophysical and geotechnical site investigation tools; including sampling, CPTU, CPTU pore pressure dissipation tests and field vane tests (FVT).

A silty, clayey sand constitutes the top soil (Unit I) and extends down to about 4.5 to 5 m depth. The geologically normally consolidated clayey silt below (Units II and III) extend down to about 15 to 16 m depth, with soil behavior type index ($I_c$) generally plotting between 2.6 and 2.95. Normalized cone resistance ($Q_t$) and pore pressure ratio ($B_q$) in these soil units are generally in the order of 7.5 and 0.1 – 0.3, respectively. The silt is uniform and structureless to mottled, with primary bedding and laminations almost absent due to bioturbation. Both Units II and III contain similar amounts of quartz (40%), plagioclase (30%), feldspar (12%), clay minerals and mafic minerals (amphibole). Clay minerals are illite and chlorite, and the presence of expanding clay minerals are low or absent. Unit IV, a low to medium strength clay has a slightly laminated structure, with occasional shell fragments and drop stones. $Q_t$ and $B_q$ are generally in the order of 4 and 0.8 – 1.0, respectively. Depth to bedrock dips sharply from the northeast to southwest but is typically identified at 21 m depth in the southern part of the site. Table 1 and Figure 3 summarizes typical soil properties and CPTU characteristics of the silt at 11.3 m and clay at 17.8 m depth.

**Table 1.** Typical soil properties at Halden Research site, 11.3 m and 17.8 m depth.

| $z$ | $w$ | $e_i$ 1) | $w_L$ 2) | $I_p$ | Fines 3) | Clay 3) | $c_{v0}$ 4) |
|---|---|---|---|---|---|---|---|
| [m] | [m] | [-] | [%] | [%] | [%] | [%] | [m²/yr] |
| 11.5 | 27 | 0.73 | 23 | 1 | 89 | 9 | 221 |
| 18.6 | 34 | 0.96 | 27 | 9 | 87 | 28 | 10 |

1) $e_i$ = initial void ratio. Note also $e_{max}$ = 1.51 and $e_{min}$ = 0.60, giving an estimated relative density, $D_r$ = 86% for $z$ = 11.3 m;
2) Liquid limit determined by the Casagrande cup;
3) Fines < 0.063 mm, clay < 0.002 mm;
4) Coefficient of vertical consolidation at $\sigma'_{v0}$.

# 4. Results

## 4.1. Triaxial testing

The CAUC clay specimen from 18.6 m depth had a volumetric recompression strain of $\varepsilon_{vol}$ = 2.7%, corresponding to $\Delta e/e_0$ = 0.054, thus giving it a "good to fair" sample quality rating [42]. During shear the specimen showed a peak shear stress and exhibited strain softening thereafter. The undrained shear strength indicated from this test was $s_{uC}$ = 82 kPa at a vertical strain of $\varepsilon_{vf}$ = 0.8%. The pore pressure at peak shear stress was 35 kPa corresponding to a Skempton's pore pressure parameter $A_f$ = 0.59 at failure (Figure 4). Interestingly, the effective stress path tags the failure envelope defined by the $K_f$ line of the CAUC tests conducted in the silt units, indicated by the maximum obliquity friction angle $\phi'_{mo}$ = 35.8° [8].

The CAUC silt specimen from 8.4 m, 11.5 m and 12.6 m depth [8] had recompression metrics of $\varepsilon_{vol}$ = 1.3%, 1.0% and 1.1% for volumetric strain and $\Delta e/e_0$ = 0.029, 0.023 and 0.026, respectively. By the clay-based sample quality framework these low values of $\Delta e/e_0$ would rate the specimens as "good to excellent" sample quality [42, 43]. However, the clay-based sample quality criteria have been shown to be misleading for low plasticity silts [4, 44]. Figure 4 shows that, except for the initial contractive type behavior, the specimens develop net negative pore pressure changes, and thus, show a strong tendency towards dilative behavior. The test results show a distinct initial S-shape behavior in stress-path space, particularly for the specimens sampled at 8.4 m and 11.5 m depth. Phase transformation points (PTP), i.e., the point at which the soil transitions from contractive type behavior to dilative type behavior, are located at an angle of approximately $\phi'_{PTP}$ = 33°. The stress-path results generally track the $K_f$ line at a maximum obliquity friction angle $\phi'_{mo}$ = 35.8° [8] to the end of the test. Due to this strain hardening behavior interpretation of the undrained shear strength from these CAUC tests is complex and the

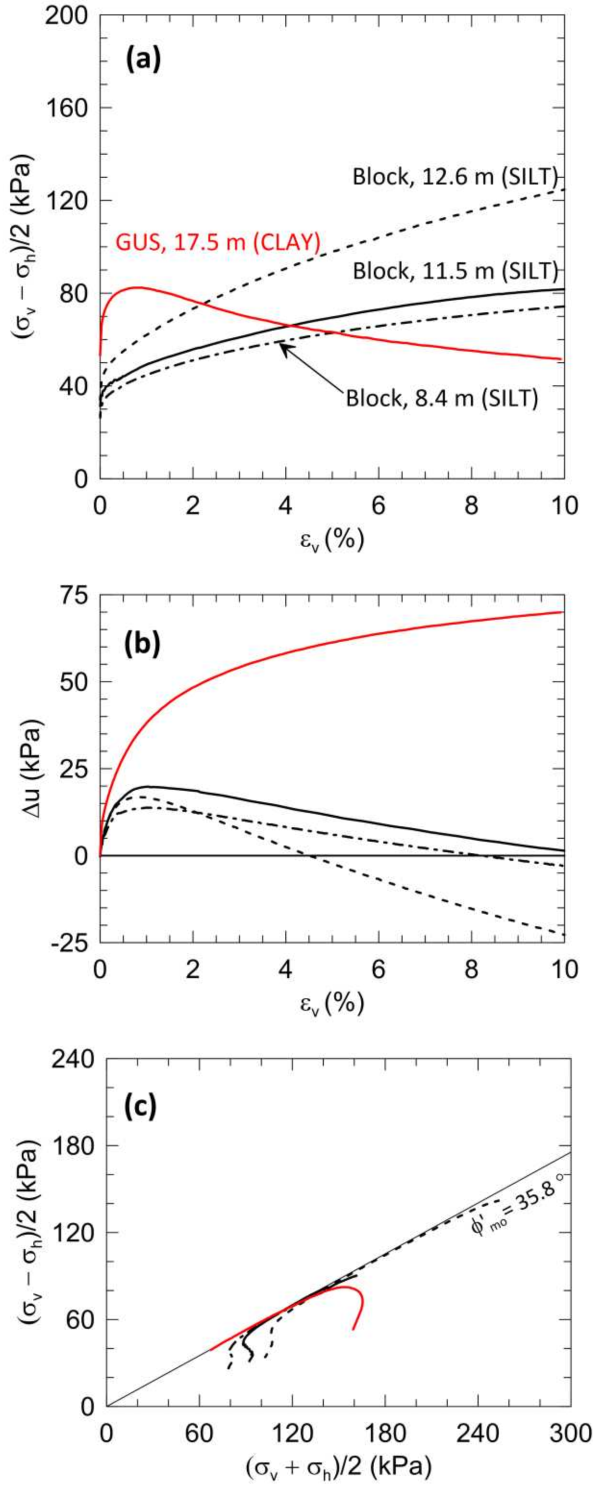


**Figure 4.** Undrained triaxial test results (CAUC) from the Halden clay and silt units.

results provide no unique (peak) undrained shear strength. Undrained shear strength evaluated at different criteria [41] are presented in Table 2.

## 4.2. Screw plate load testing

### 4.2.1. Load-displacement behavior

Typical stress - displacement curves from the silt (11.3 m) and clay (17.8 m) tests are presented in Figure 5. The SPLT results from the clay shows a distinct change in displacement around $q_p$ = 400 kPa and relatively large displacements for small changes in load thereafter. The results of the two silt tests show more gradual increase in deformation with load. The tests exhibit a significantly more pronounced strain-hardening relative to the clay test - similar to the triaxial test results described above. There is reasonable agreement between the two tests conducted at 11.3 m depth in boreholes HALSP01 and HALSP02, although some variability is evident. All tests were stopped at a displacement corresponding to about 0.2$D$.

Although traditionally calculated for CPTU twitch tests [1], an assessment of normalized penetration velocity gives $V$ = 10 for the SPLT in the clay unit (assuming $c_h$ = $c_{v0}$, Table 1) indicating that undrained conditions prevailed, as expected. From the load tests in the silt unit, the normalized penetration velocity is about $V$ = 0.5, and thus, suggests partially drained conditions during loading. These conditions cause complex pore pressure fields surrounding the screw plate, with large gradients in the vertical direction. Locally near the plate the soil shear resistance is fully mobilized and likely developed negative pore pressure changes combined with some dilation due to partial drainage. Whereas at some distance below the plate (and radially), soil elements may have experienced positive pore pressure changes combined with some contraction due to the increase in compression stresses being greater than the mobilized shear stresses (resulting in the soil remaining well below the failure envelope). Globally, however, the load-displacement behavior of the silt tests suggests a dilative type of behavior, with stresses acting on the screw plate increasing at a significantly larger rate relative to the test in clay.

### 4.2.2. Bearing capacity

Ultimate bearing capacities from the SPLTs were assessed using three different criteria as detailed above and illustrated for each individual SPLT on Figure 5. The bearing capacity interpreted at a displacement equal to 10% of the plate diameter, gave consistently higher values, i.e. $q_{0.1D}$ > $q_{TI}$, $q_{KP}$, relative to the other two criteria. The tangent intersect and Kay and Parry [15] interpretation methods gave similar values of $q_{ult}$ in both the silt and clay units (Table 3).

### 4.2.3. Undrained shear strength

The back-calculated undrained shear strength in the clay from $q_{0.1D}$, $q_{TI}$ and $q_{KP}$ (Eq. (4)) gave values of $s_u$ = 54 kPa, 46 kPa and 47 kPa, respectively (Table 2) when applying a bearing capacity factor of $N_c^*$ = 9. These values are considered "average" or "mobilized" undrained shear strengths for the soil at the screw plate embedment depth, thus approximately equivalent to the direct simple shear (DSS) undrained shear strength ($s_{uD}$) of the same soil. The DSS and CAUE undrained shear strengths of the Halden clay can be estimated as $s_{uD}$ = 57 kPa and $s_{uE}$ = 34 kPa, respectively, based on the strength anisotropy factors $s_{uD}/s_{uC}$ = 0.69 and $s_{uE}/s_{uC}$ = 0.42 reported by Lunne, et al. [42] for similar clays from the Oslo, Norway area. Thus, the undrained shear strength back-calculated from $q_{0.1D}$ provides excellent agreement (within 5%) with the laboratory test and strength anisotropy of the region,

**Table 2.** Apparent and measured undrained shear strength from screw plate load tests, field vane and triaxial tests at Halden.

| Type [-] / $z$ [m] | 11.3 – 11.5 (silt) [kPa] | 17.8 – 18.5 (clay) [kPa] |
|---|---|---|
| *Laboratory CAUC* | | |
| $s_{u,C}$ [$(\sigma_1 - \sigma_3)_{max}$] | 94 | 82 |
| $s_{u,C}$ ($u_{max}$) | 50 | - |
| $s_{u,C}$ ($\varepsilon_{vf}$ = 2%) | 57 | - |
| $s_{u,C}$ ($A_f$ = 0) | 84 | - |
| $s_{u,C}$ [$(\sigma_1/\sigma_3)_{max}$] | 70 | - |
| $s_{u,C}$ ($K_f$) | 70 | - |
| $s_{u,C}$ ($\varepsilon_{vf}$ = 10%) | 84 | - |
| *In situ tests* | | |
| $s_{u,TI}$ | 72 [1)] | 46 |
| $s_{u,0.1D}$ | 92 [1)] | 54 |
| $s_{u,KP}$ | 64 [1)] | 47 |
| $s_{u,FVT}$ | 45 | 41 |
| $s_{u,SBP}$ | 51 | - |
| **Note:** [1)] Average of two tests | | |

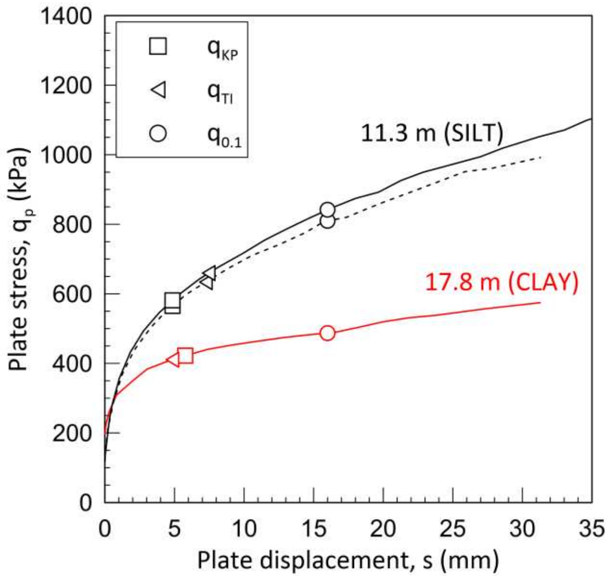


**Figure 5.** Typical stress-displacement curves from screw plate load tests in the silt (11.3 m) and clay (17.8 m) units at Halden. Ultimate bearing stress assessed using the 0.1D, ($q_{0.1D}$), tangent intersect ($q_{TI}$) and Kay and Parry ($q_{KP}$) methods.

**Table 3.** Bearing capacity interpreted from screw plate load tests at 11.3 m and 17.8 m depth.

| **Borehole** | **Depth** | **TI** | **0.1D** | **KP** |
|---|---|---|---|---|
| **[-]** | **[m]** | **[kPa]** | **[kPa]** | **[kPa]** |
| HALSP01 | 11.3 | 634 | 810 | 566 |
| HALSP02 | 11.3 | 660 | 842 | 581 |
| HALSP02 | 17.8 | 410 | 487 | 422 |

and validates both the SPLT stress-displacement results and the equipment as an effective tool for evaluation of undrained shear strength in soft clay. FVT results at the same depth [8] resulted in $s_{u,FVT}$ = 41 kPa (i.e. $s_{u,FVT}/s_{uC}$ = 0.5), and thus show better agreement with the back-calculated undrained shear strength using $q_{TI}$.

Drainage conditions during the SPLTs in the silt unit are complex and uncertain, but as noted above the tests were likely partially drained ($V$ = 0.5). However, back-calculation of in situ strength parameters using conventional methods requires an assumption of the prevailing conditions as either drained or undrained during loading. By assuming undrained conditions $s_u$ of the silt was back-calculated using Eq. (4). Table 2 presents the results from these back-calculations, in terms of average $s_{u,TI}$, $s_{u,0.1D}$ and $s_{u,KP}$ representing the undrained shear strength calculated from $q_{TI}$, $q_{0.1D}$ and $q_{KP}$, respectively. Interestingly, the TI and KP results (72 kPa and 64 kPa) show agreement with the CAUC test at the same depth level for $s_{uC}$ interpreted using the shear stress at the $K_f$ line and at maximum obliquity criteria (70 kPa). It is hypothesized that the SPLT tests in the silt do generate negative pore pressures changes, and that the TI (≈ KP) failure criteria represent the point at which the soil elements involved in the global failure mechanism below the plate start becoming fully mobilized. Furthermore, the undrained shear strengths back-calculated from $q_{0.1D}$ ($s_{u,0.1D}$ = 92 kPa) show similarities with the undrained strength interpreted at $(\sigma_1 - \sigma_3)_{max}$ of the companion CAUC test ($s_{uC}$ = 94 kPa). This implies that the shear stress obtained from CAUC tests on silt block sample specimens at large strains can be used to reliably estimate the bearing capacity at 0.1$D$ for short term loading and that the strain hardening effect can be relied upon. This, however, requires high quality samples with minimum of sample disturbance from sampling, transportation and handling. Recent studies have shown that effects of disturbance on silt samples can have opposite effects of that often seen for structured clays, i.e., larger interpreted strength and stiffness properties with increasing disturbance [4, 44].

### 4.2.4. Effective stress friction angle

For back-calculation of the effective stress friction angle of the silt using conventional methods drained conditions are required. By assuming fully drained conditions during SPLT loading $\phi'$ were estimated using the stress-displacement curve and Eq. (3). The largest uncertainty in this back-calculation is the bearing capacity factor, $N_q^*$, which varies significantly in the literature [45, 46] (Figure 6). The bearing capacity factor computed from the SPLTs at 11.3 m depth are failure criteria dependent, but range between $N_q^*$ = 4.3 and 6.5, resulting in corresponding values of $\phi'$ = 12° – 24° using the curves in Figure 6. Effective stress friction angles in this range are considered unrealistically low compared to results from triaxial tests conducted specimens of Halden silt and other international silts reported in literature [7, 19, 41, 47-49]. This implies that the SPLTs were not fully drained during loading, i.e. partial drainage prevailed as suggested by $V$ = 0.5, and that the measured bearing capacities cannot be used to reliably back-calculate the friction angle. The bearing capacity factor appear highly uncertain in silts. Helical Anchors Inc. [50] suggests $N_q^*$ = 28 for compression loading of a helical pile in a cohesionless soil and hence with an effective stress friction angle of $\phi'_{mo}$ = 35.8°, overestimates the ultimate bearing capacity (unfactored) of the screw plate load tests at 11.3 m depth by factors of 3.5 to 5.5. Using the constant volume friction angle (approximately equal to $\phi'_{PTP}$) of $\phi'_{cv}$ = 33° reduces the corresponding value of $N_q^*$ to about 19.

The Canadian foundation engineering manual [33] presents typical bearing capacity factors for deep foundations in silt as 10 – 30 (cast-in-place piles) and 20 – 40 (driven piles), and as a result, also overpredicts $q_{ult}$. For offshore piles in cohesionless soils API RP2A [31] suggests $N_q^*$ in the range of 8 – 12 for medium dense to dense silts, giving better agreement with the SPLT bearing capacity results. However, predictions of axial capacity of piles driven into cohesionless soil using API RP2A have been noted to be inaccurate [36, 51] and more recent guidelines [e.g. 52] recommend CPTU-based methods to assess bearing capacity in these soils.

## 5. Measured and calculated capacity

Figure 7 presents the measured SPLT bearing capacity at $s = 0.1D$ displacement ($q_{0.1D}$) plotted with ultimate unit base resistance ($q_{b,ult}$) of an equivalent diameter closed end pile using clay methods at 17.8 m depth and cohesionless soil (sand) methods for the silt at 11.3 m depth. In the clay the measured SPLT result shows excellent agreement with the calculated bearing capacity using $N_c^*$ = 9 and a DSS undrained shear strength, $s_{uD}$, as noted in Section 4.2.3 above. The API RP2A and NGI-05 methods use the unconsolidated undrained shear strength ($s_{uUU}$), in this case assumed equal to $s_{uC}$, and appear to overestimate the capacity by about 50%. The ICP/MTD-1996 and UWA-13 methods (using corrected cone resistance, $q_t$) also overestimate the capacity in the clay, by a factor of 1.33. Helical Anchors Inc. [50] do not state what undrained shear strength to use for design but for illustration purposes $s_{uD}$ was used in Figure 7 for calculation of $q_{b,ult}$. CGS [33] suggests the minimum undrained shear strength (i.e., $s_{uE}$) for capacity assessment, and as a result $q_{b,ult}$ is underestimated relative to $q_{0.1D}$. In summary, the best agreement with the measured bearing capacity of the SPLT at $0.1D$ in the Halden clay was obtained by using $s_{uD}$ and a bearing capacity factor equal to 9.

Relative to the measured values of $q_{0.1D}$, the classic drained bearing capacity equation for deep foundations in cohesionless soil typically over estimates the unit base resistance at Halden by a factor of up to 4.5, but the values of $q_{b,ult}$ are highly dependent on the selected bearing capacity factor, $N_q^*$. For example, API RP2A using $N_q^*$ = 8 shows fair agreement with the measured values from the SPLTs. The CPTU-based methods all underestimate the unit base resistance at 10% vertical displacement. It should be noted, however, that these methods were developed for sands with significantly higher cone resistances and that CPTU $q_c$ at 11.3 m depth at Halden were measured using the conventional penetration rate of 20 mm/s, giving normalized velocities of about $V = 180$ [53], i.e., fully undrained conditions. Furthermore, relative density ($D_r$) derived from $q_c$ and estimated effective horizontal stresses, $\sigma'_h$ [54], were developed for clean sands. $D_r$ estimates at Halden (80% - 86%) were based on measured initial void ratios ($e_i$) of seven triaxial specimens trimmed from a block sample collected at 11.5m depth and maximum and minimum void ratios measured on air dried silt from the same block sample (Table 1). Values of $q_c$ and $D_r$ used in the CPTU-based methods for calculation of $q_{b,ult}$ are therefore somewhat uncertain.

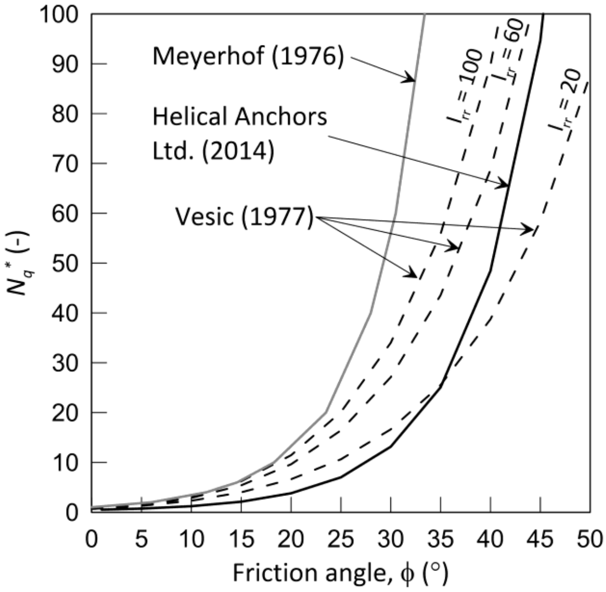


**Figure 6.** Bearing capacity factors, $N_q^*$ for deep foundations in cohesionless soil as function of effective stress friction angle.

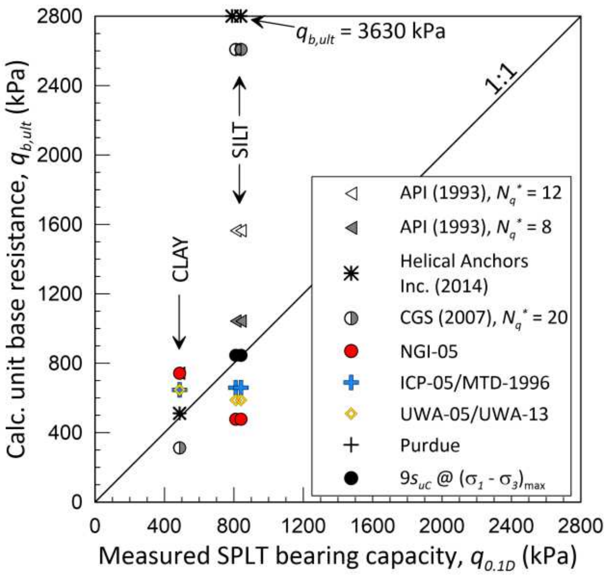


**Figure 7.** Measured SPLT bearing capacity ($q_{0.1D}$) versus calculated base unit resistance of an equivalent closed end pile ($q_{b,ult}$).

## 6. Summary and conclusions

The screw plate load test (SPLT) was considered an attractive tool for investigation of the in situ soil behavior of the silt deposit at Halden, Norway described by Blaker, et al. [8], which displays dilative type behavior during undrained shear in the laboratory CAUC tests and a maximum obliquity friction angle of $\phi'_{mo} = 35.8°$. One test was conducted in the clay unit below 16 m depth and two companion tests were performed in the silt at 11.3 m depth. The main findings were:

- The SPLT in the clay were conducted with a normalized velocity of about $V = 10$, indicating undrained conditions during loading. The soil displayed a distinct break in the stress - displacement curve during loading.
- Interpretation of the clay test confirmed (within 5%) the theoretical bearing capacity estimated using the direct simple shear (DSS) undrained shear strength of the same soil, thus validating the

stress-displacement curve and the equipment as an effective tool for evaluation of undrained shear strength in soft clay.

- The two SPLTs performed in silt showed good repeatability and a normalized velocity of about 0.5. Normalized velocities in the range 10 > $V$ > 0.05 have been suggested to be indicative of partially drained conditions. Thus, the rate of loading used at Halden likely caused complex pore pressure fields surrounding the screw plate.
- Both silt tests displayed a significantly more pronounced strain-hardening behavior relative to the clay SPLT. This behavior confirmed the observations from the stress-strain and stress-path development during undrained triaxial shearing (CAUC) of the bock sample from the same depth.
- Due to the strain hardening effect the bearing capacities at a displacement equal to 0.1$D$ gave consistently higher values relative to the tangent intersect and Kay and Parry [15] methods.
- It is suggested that the SPLT generated negative pore pressure changes in the silt immediately below the plate, and that $q_{ult}$ for the tangent intersect criteria represents the start of a fully mobilized shear stress state below the screw plate, equivalent to the $K_f$ and maximum obliquity failure criteria used for assessment of $s_u$ from CAUC tests.
- The negative shear induced pore pressures and undrained shear strength at large strains observed from CAUC testing on the silt block sample can likely be relied upon for short term loading in the field. For extrapolation to other silt sites one must ensure high quality samples for laboratory testing and that the effects of disturbance on the engineering design parameter are properly evaluated.
- Fully drained bearing capacities were likely not measured during the SPLTs at Halden. The bearing capacity factor is a function of effective stress friction angle and, as a result Eq. (3) typically over predict $q_{ult}$ at Halden. Similarly, as an effect of the undrained response and relatively low values of cone resistance the CPTU-based methods for estimation of $q_{ult}$ under predict the bearing capacity.

## Acknowledgements

This study has primarily been financed by the Norwegian Geotechnical Institute (NGI) and the Research Council of Norway (RCN) under Grant No. 245650. The field vane tests were conducted with support from the US National Science Foundation (NSF) under Grant Nos. CMMI-1436793 and CMMI-1436617. Any opinions, findings, and conclusions or recommendations expressed in this material are those of the author(s) and do not necessarily reflect the views of NGI, RCN or NSF. This support is gratefully acknowledged.

## References

[1] Randolph, M.F., "Characterization of Soft Sediments for Offshore Applications", in Geotechnical and Geophysical Site Characterization, A. Viana da Fonseca and P.W. Mayne, (eds.). 2004, Millpress: Rotterdam, The Netherlands. p. 209–232.

[2] DeJong, J.T. and M. Randolph, "Influence of Partial Consolidation during Cone Penetration on Estimated Soil Behavior Type and Pore Pressure Dissipation Measurements". Journal of Geotechnical and Geoenvironmental Engineering, 2012. **138**(7): p. 777-788 https://doi.org/10.1061/(ASCE)GT.1943-5606.0000646.

[3] Kim, K., M. Prezzi, R. Salgado, and W. Lee, "Effect of Penetration Rate on Cone Penetration Resistance in Saturated Clayey Soils". Journal of Geotechnical and Geoenvironmental Engineering, 2008. **134**(8): p. 1142-1153 https://doi.org/10.1061/(ASCE)1090-0241(2008)134:8(1142).

[4] Carroll, R. and M. Long, "Sample Disturbance Effects in Silt". Journal of Geotechnical and Geoenvironmental Engineering, 2017. **143**(9): p. 04017061 https://doi.org/10.1061/(ASCE)GT.1943-5606.0001749.

[5] Fleming, L.N. and J.M. Duncan, "Stress-Deformation Characteristics of Alaskan Silt". Journal of Geotechnical Engineering, 1990. **116**(3): p. 377-393 https://doi.org/10.1061/(asce)0733-9410(1990)116:3(377).

[6] Høeg, K., R. Dyvik, and G. Sandbækken, "Strength of undisturbed versus reconstituted silt and silty sand specimens". Journal of Geotechnical and Geoenvironmental Engineering, 2000. **126**(7): p. 606-617 https://doi.org/10.1061/(asce)1090-0241(2000)126:7(606).

[7] Long, M., G. Gudjonsson, S. Donohue, and K. Hagberg, "Engineering characterisation of Norwegian glaciomarine silt". Engineering Geology, 2010. **110**(3): p. 51-65 https://doi.org/10.1016/j.enggeo.2009.11.002.

[8] Blaker, Ø., R. Carroll, P. Paniagua, D.J. DeGroot, and J.-S. L'Heureux, "Halden research site: geotechnical characterization of a post glacial silt". AIMS Geosciences, 2019. **5**(2): p. 184-234 https://doi.org/10.3934/geosci.2019.2.184.

[9] Marsland, A., "Clays subjected to in situ plate tests". Ground Engineering, 1972. **5**(6): p. 24-31.

[10] Kummeneje, O., "Fundamentering av oljetank i Drammen (Foundation of an oil tank in Drammen)". Norwegian Geotechnical Institute Publication (In [Norwegian]), 1956. **12**: p. 1-6.

[11] Schmertmann, J.H., "Static Cone to Compute Static Settlement over Sand". Journal of the Soil Mechanics and Foundations Division, ASCE, 1970. **96**(SM3): p. 1011-1043.

[12] Dahlberg, R., "Settlement characteristics of preconsolidated natural sands: In-situ screw-plate, pressurementer and penetration tests". 1975, National Swedish Institute for Building Research: Stockholm, Sweden. p. 315.

[13] Bergado, D. and N. Huan, "Undrained Deformability and Strength Characteristics of Soft Bangkok Clay By the Screw Plate Test". Geotechnical Testing Journal, 1987. **10**(3): p. 113-122 https://doi.org/10.1520/GTJ10943J.

[14] Bergado, D.T., K.C. Chong, P.A.M. Daria, and M.C. Alfaro, "Deformability and consolidation characteristics of soft Bangkok clay using screw plate tests". Canadian Geotechnical Journal, 1990. **27**(5): p. 531-545 https://doi.org/10.1139/t90-069.

[15] Kay, J.N. and R.H.G. Parry, "Screw plate tests in a stiff clay". Ground Engineering, 1982. **15**(6): p. 22-27.

[16] Selvadurai, A.P.S., G.E. Bauer, and T.J. Nicholas, "Screw plate testing of a soft clay". Canadian Geotechnical Journal, 1980. **17**(4): p. 465-472 https://doi.org/10.1139/t80-055.

[17] Kay, J.N. and D.L. Avalle, "Application of Screw Plate to Stiff Clays". Journal of the Geotechnical Engineering Division, ASCE, 1982. **108**(GT1): p. 145-154.

[18] Janbu, N. and K. Senneset, "Field compressometer - principles and applications", in Eighth International Conference on Soil Mechanics and Foundation Engineering, N.A. TsytovichN and S. Chetyrkin, (eds.). 1973. p. 191-198.

[19] Sandven, R., "Geotechnical properties of a natural silt deposit obtained from field and laboratory tests", in Characterisation and Engineering Properties of Natural Soils, T.S. Tan, et al., (eds.). 2003, A.A. Balkema: Lisse. p. 1121–1148.

[20] Lefebvre, G. and C. Poulin, "A new method of sampling in sensitive clay". Canadian Geotechnical Journal, 1979. **16**(1): p. 226-233 https://doi.org/10.1139/t79-019.

[21] Andresen, A. and P. Kolstad, "The NGI 54-mm samplers for undisturbed sampling of clays and representative sampling of coarser materials", in Proc., Int. Symp. of Soil Sampling, State of the Art on Current Practice of Soil Sampling. 1979, Japanese Society of Soil Mechanics and Foundation Engineering: Tokyo, Japan. p. 13-21.

[22] Strout, J.M., "Evaluation of the field compressometer test in sand", Ph.D., The Norwegian University of Science and Technology, 1998.
[23] Lacasse, S. and T. Berre, "State-of-the-Art: Triaxial testing methods for soils", in Advanced Triaxial Testing of Soil and Rock, ASTM STP 977, R. Donaghe, R. Chaney, and M. M. Silver, (eds.). 1988, ASTM International: West Conshohocken, PA. p. 264-289.
[24] Ladd, C.C. and D.J. DeGroot, "Recommended practice for soft ground site characterization: Arthur Casagrande lecture", in Proc., 12th Panamerican Conf. on Soil Mech. and Geotech. Eng., P.J. Culligan, H.H. Einstein, and A.J. Whittle, (eds.). 2003, Verlag Glückauf: Essen, Germany. p. 1-55.
[25] Berre, T., "Triaxial Testing at the Norwegian Geotechnical Institute". Geotechnical Testing Journal, 1982. **5**(1/2): p. 3-17 https://doi.org/10.1520/GTJ10794J.
[26] Briaud, J.-L. and P. Jeanjean, "Load settlement curve method for spread footings on sand", in Vertical and Horizontal Deformations of Foundations and Embankments, GSP 40, A.T. Yeung and G.Y. Félio, (eds.). 1994, ASCE: New York, NY. p. 1774-1804.
[27] Salgado, R., S.I. Woo, and D. Kim, "Development of Load and Resistance Factor Design for Ultimate and Serviceability Limit States of Transportation Structure Foundations". 2011, Joint Transportation Research Program, Indiana Department of Transportation and Purdue University: West Lafayette, IN, USA.
[28] Trautmann, C.H. and F.H. Kulhawy, "Uplift Load-Displacement Behavior of Spread Foundations". Journal of Geotechnical Engineering, 1988. **114**(2): p. 168-184 https://doi.org/10.1061/(ASCE)0733-9410(1988)114:2(168).
[29] De Beer, E.E., "Experimental Determination of the Shape Factors and the Bearing Capacity Factors of Sand". Géotechnique, 1970. **20**(4): p. 387-411 https://doi.org/10.1680/geot.1970.20.4.387.
[30] Salgado, R., "The Engineering of Foundations". 2008, Boston, MA, USA: McGraw Hill.
[31] API, "Recommended practice for planning, designing and constructing fixed offshore platforms – working stress design. API RP 2A-WSD, 20th Edition". 1993, American Petroleum Institute: Washington, DC, USA.
[32] Bowles, J.E., "Foundation Analysis and Design". 1996, New York: McGraw-Hill.
[33] CGS, "Canadian Foundation Engineering Manual, 4th edition". 2007, Canadian Geotechnical Society: Richmond, B.C., Canada.
[34] Clausen, C.J.F., P.M. Aas, and K. Karlsrud, "Bearing Capacity of Driven Piles in Sand, the NGI Approach", in Proc. of the 1st Int. Symp. on Frontiers in Offshore Geotech., S. Gourvenec and M. Cassidy, (eds.). 2005, Taylor & Francis: London. p. 677-682.
[35] Karlsrud, K., C.J.F. Clausen, and P.M. Aas, "Bearing Capacity of Driven Piles in Clay, the NGI Approach", in Proc. of the 1st Int. Symp. on Frontiers in Offshore Geotech., S. Gourvenec and M. Cassidy, (eds.). 2005, Taylor & Francis: London. p. 775-782.
[36] Jardine, R.J. and F.C. Chow, "New Design Methods for Offshore Piles". MTD Publication. Vol. 96/103. 1996, London: Marine Technology Directorate. 48.
[37] Jardine, R.J., F.C. Chow, R. Overy, and J. Standing, "ICP Design Methods for Driven Piles in Sand and Clay". 2005, London: Thomas Telford Publishing.
[38] Lehane, B.M., J.A. Schneider, and X. Xu, "The UWA-05 Method for Prediction of Axial Capacity of Driven Piles in Sand", in Proc. of the 1st Int. Symp. on Frontiers in Offshore Geotech., S. Gourvenec and M. Cassidy, (eds.). 2005, Taylor & Francis: London. p. 683-689.
[39] Lehane, B.M., Y. Li, and R. Williams, "Shaft Capacity of Displacement Piles in Clay Using the Cone Penetration Test". Journal of Geotechnical and Geoenvironmental Engineering, 2013. **139**(2): p. 253-266 https://doi.org/10.1061/(ASCE)GT.1943-5606.0000749.
[40] Han, F., M. Prezzi, R. Salgado, and M. Zaheer, "Axial Resistance of Closed-Ended Steel-Pipe Piles Driven in Multilayered Soil". Journal of Geotechnical and Geoenvironmental Engineering, 2017. **143**(3): p. 04016102 https://doi.org/10.1061/(ASCE)GT.1943-5606.0001589.
[41] Brandon, T.L., A.T. Rose, and J.M. Duncan, "Drained and undrained strength interpretation for low-plasticity silts". Journal of Geotechnical and Geoenvironmental Engineering, 2006. **132**(2): p. 250-257 https://doi.org/10.1016/(asce)1090-0241(2006)132:2(250).
[42] Lunne, T., T. Berre, K.H. Andersen, S. Strandvik, and M. Sjursen, "Effects of sample disturbance and consolidation procedures on measured shear strength of soft marine Norwegian clays". Canadian Geotechnical Journal, 2006. **43**(7): p. 726-750 https://doi.org/10.1139/t06-040.
[43] Lunne, T., P.K. Robertson, and J.J.M. Powell, "Cone penetration testing in geotechnical practice". 1997, London: Blackie Academic & Professional.
[44] Lukas, W.G., D.J. DeGroot, J.T. DeJong, C.P. Krage, and G. Zhang, "Undrained Shear Behavior of Low-Plasticity Intermediate Soils Subjected to Simulated Tube-Sampling Disturbance". Journal of Geotechnical and Geoenvironmental Engineering, 2019. **145**(1): p. 04018098 https://doi.org/10.1061/(ASCE)GT.1943-5606.0001967.
[45] Meyerhof, G.G., "Bearing Capacity and Settlement of Pile Foundations". Journal of the Geotechnical Engineering Division, ASCE, 1976. **102**(GT3): p. 195-228.
[46] Vesic, A.S., "Design of pile foundations". 1977, National Cooperative Highway Research Program Synthesis of Highway Practice No. 42: Washington, D.C., USA.
[47] Cola, S. and P. Simonini, "Mechanical behavior of silty soils of the Venice lagoon as a function of their grading characteristics". Canadian Geotechnical Journal, 2002. **39**(4): p. 879–893 https://doi.org/10.1139/t02-037.
[48] Nocilla, A., M.R. Coop, and F. Colleselli, "The mechanics of an Italian silt: an example of 'transitional' behaviour". Géotechnique, 2006. **56**(4): p. 261-271 https://doi.org/10.1680/geot.2006.56.4.261.
[49] Long, M., "Engineering characterization of estuarine silts". Quarterly Journal of Engineering Geology and Hydrogeology, 2007. **40**: p. 147-161 https://doi.org/10.1144/1470-9236/05-061.
[50] Helical Anchors Inc., "Engineering Design Manual, Rev 02". 2014, Helical Anchors, Inc.: Minneapolis, MN, USA.
[51] Randolph, M.F., R. Dolwin, and R. Beck, "Design of driven piles in sand". Géotechnique, 1994. **44**(3): p. 427-448 https://doi.org/10.1680/geot.1994.44.3.427.
[52] API, "Geotechnical and Foundation Design Considerations. ANSI/API Recommended Practice 2GEO 1st edition, April 2011. ISO 19901-4:2003 (Modified), Petroleum and natural gas industries - Specific requirements for offshore structures, Part 4 - Geotechnical and foundation design considerations". 2011, American Petroleum Institute: Washington, DC, USA.
[53] Carroll, R. and A.P. Paniagua López, "Variable rate of penetration and dissipation test results in a natural silty soil", in Cone Penetration Testing 2018: Proc. of the 4th Int. Symp. on Cone Penetration Testing, M.A. Hicks, F. Pisanò, and J. Peuchen, (eds.). 2018, CRC Press: London.
[54] Jamiolkowski, M., D.C.F.L. Presti, and M. Manassero, "Evaluation of Relative Density and Shear Strength of Sands from CPT and DMT", in Geotechnical Special Publication No. 119: Soil Behavior and Soft Ground Construction, J.T. Germaine, T.C. Sheahan, and R.V. Whitman, (eds.). 2003, American Society of Civil Engineers: Reston, VA. p. 201-238.